Roton backflow and quasiparticle scattering at ^{4}He surfaces

M. B. Sobnack,[1] J. R. Matthias,[2] J. C. H. Fung,[3] C. D. H. Williams,[2] and J. C. Inkson[2]
[1]*Condensed Matter Theory Group, Department of Physics, Loughborough University, Loughborough, Leicestershire LE11 3TU, United Kingdom*
[2]*School of Physics, University of Exeter, Stocker Road, Exeter EX4 4QL, United Kingdom*
[3]*Department of Mathematics, The Hong Kong University of Science and Technology, Clear Water Bay, Kowloon, Hong Kong, China*
(Received 6 July 2001; revised manuscript received 18 September 2001; published 7 May 2002)

We study the effect of roton backflow on the scattering of quasiparticles and atoms at the free surface of superfluid ^{4}He at $T=0$ K. As a starting point, we use Beliaev's formalism and include backflow semiphenomenologically in the form of a backflow potential. We derive equations of motion for the bulk quasiparticles and the free atoms. Assuming that all the quasiparticles travel ballistically, we solve the equations of motion numerically for oblique incidence and calculate probabilities for all the one-to-one surface scattering processes allowed by the conservation laws. We compare the results with those obtained when backflow is neglected. Use of some of the calculated rates in the simulations of experiments shows that the calculated scattering rates with backflow included are in improved agreement with experiments.

DOI: 10.1103/PhysRevB.65.184521 PACS number(s): 67.40.Db

I. INTRODUCTION

Since its discovery,[1] the superfluidity of ^{4}He has been a topic of considerable interest, largely because of the fact that it is an ideal system on which to test the fundamental concepts of quantum mechanics. One of the principal notions of a many-body system in the quantum regime is that of Landau's quasiparticles,[2] which holds that the excited states of the fluid should exhibit particlelike properties. That this is the case has long been established by neutron-scattering experiments.[3] The interaction between these quasiparticles and the free surface of a superfluid sample, giving rise to the evaporation of atoms into the vapor, has recently been investigated in a number of experiments.[4–10] These experiments have been developed to such a degree that they now provide a good means of probing the nature of the quasiparticles[10] and how they interact with one another.

At low temperatures, superfluid ^{4}He exhibits the peculiar phenomenon of quantum evaporation. Elementary excitations propagate in the liquid with long mean free paths and with an energy that can exceed the binding energy of the atoms in the liquid. When such an excitation impinges on the free surface it may eject an atom through a quantum process. The process of quantum evaporation and the reverse process of quantum condensation have been studied extensively over the years. Wyborn and Wyatt[9] established that the processes conserve energy and momentum parallel to the surface. One of the difficulties with experiments on quantum evaporation is in the calibration of the detectors; for various reasons, it is difficult for experimentalists to deduce absolute values for the probabilities of quasiparticle evaporation. This emphasizes the need for theoretical predictions.

Over the years, there have been several theoretical studies[11–19] of one-to-one quasiparticle scattering at the free surface. Recently, Sobnack and co-workers[20–22] adapted Beliaev's theory[23] to the inhomegeneous superfluid ^{4}He system with a free surface at $T=0$ K and calculated probabilities for the one-to-one surface scattering processes as a function of energy. The use of their calculated probabilities in simulations of experiments[20,22,24] showed that, while the calculated probability of evaporation by phonons show very good agreement with experiments, the calculations underestimate the evaporation efficiencies of R^+ rotons—the probabilities were too small at low roton energies, thus highlighting the need for a better description of the roton and a better theory.

One of the physical ingredients not present in Beliaev formalism is roton backflow. The concept of backflow was introduced by Feynman and Cohen[25] when it was realized that the roton minimum was too high in the earlier Feynman theory.[26] It has subsequently become accepted that roton backflow should be considered in order to have a quantitative and physical understanding of the excitations in superfluid helium. One would, therefore, expect that backflow effects will be important at the liquid-vapor interface. In this paper, we develop a perfectly general extension of Beliaev's theory to include a semiphenomenological mean-field backflow effect by developing some of the ideas from the polarization-potential (PP) theory[27] of the 1970s. We neglect inelastic processes and assume that all the quasiparticles are stable and travel ballistically. We investigate the one-to-one scattering processes at bulk energies $\hbar\omega$ covering the range from just above the binding energy $|\mu_0|=7.16$ K to energies higher than the maxon energy $\Delta_m \sim 13.85$ K. For preliminary results of this study, see Refs. 28–30.

The paper is organized as follows. In Sec. II, we present the method we use and derive the equations of motion. The solutions to the equations are presented in Sec. III. We also give our calculated scattering rates and compare them with those published and those from experimental simulations. We conclude in Sec. IV with some remarks.

II. FORMALISM

We give briefly below the general ideas of Beliaev's theory[23] relevant to the present study. This is followed by some ideas from the polarization-potential theory of Aldrich and Pines[27] and then we discuss how we incorporate backflow into our formalism.

A. Beliaev theory

Beliaev's theory[23] is based on Bogoliubov's assumptions[31] that the condensate (the state of zero momentum) is macroscopically occupied and that the excited states are dominated by scatterings involving two condensate particles. With these assumptions, Beliaev identified that the Feynman diagrams for the system consist of three irreducible self-energy diagrams: Σ_{11}, the sum of all self-energy diagrams with equal numbers of incoming and outgoing condensate lines, Σ_{02}, the sum of all self-energy diagrams in which the number of incoming condensate lines exceeds the number of outgoing ones by two, and Σ_{20}, which has two more outgoing condensate lines than incoming ones. The superfluid ^{4}He system has two propagators, the usual single-particle Green's function $G(\mathbf{k},\omega)$ and the ''anomalous'' Green's function $F(\mathbf{k},\omega)$. The Feynman diagrams give a pair of coupled Dyson–Beliaev equations for G and F in terms of the self-energies Σ_{11}, Σ_{20}, and Σ_{02}, the condensate density ρ, and the free-particle Green's function

$$G_0(\mathbf{k},\omega)=\left[\hbar\omega-\left(\frac{\hbar^2\mathbf{k}^2}{2m}-\mu\right)+i\delta\right]^{-1}. \tag{1}$$

In the low-density (Bogoliubov) limit, the first-order diagrams for the irreducible self-energies give

$$\Sigma_{11}=\rho V(0)+\rho V(\mathbf{k}) \text{ and } \Sigma_{02}=\Sigma_{20}=\rho V(\mathbf{k}), \tag{2}$$

where $V(\mathbf{k})$ is the Fourier transform of the helium-helium potential. G and F then have poles at $\hbar\omega=\pm E_B$, where E_B is the Bogoliubov spectrum[31]

$$E_B(\mathbf{k})=\left[\frac{\hbar^4\mathbf{k}^4}{4m^2}+2\rho\frac{\hbar^2\mathbf{k}^2}{2m}V(\mathbf{k})\right]^{1/2}. \tag{3}$$

This formula gives quite a good fit to the experimentally observed spectrum if $V(k)$ is taken to be the Brueckner potential[32] $V_0k^{-1}\sin(a_0k)$, with $V_0=17.0$ K Å^{-1} and $a_0=2.26$ Å.

B. The polarization-potential theory

Aldrich and Pines[27] developed a phenomenological theory to evaluate the contribution of short-range correlations, roton backflow, and multiphonon excitations to the superfluid helium density-fluctuation spectrum at both SVP and at increased pressures. They suggested that, in analogy with plasmons in metals, the restoring force for the density oscillations may be regarded as a ''polarization potential''

$$\Phi_{\text{pol}}(\mathbf{k},\omega)=f_k^s\langle\rho(\mathbf{k},\omega)\rangle, \tag{4}$$

where f_k^s is a phenomenological parameter proportional to the strength of the induced fluctuations. In the absence of backflow and multiphonon excitations, the linear response of the system to this potential and a weak external probe, Φ_{ext}, is given by the screened density-density response function $\chi_{\text{sc}}^{\rho\rho}$, (see, for example, Ref. 33), i.e.,

$$\langle\rho(\mathbf{k},\omega)\rangle=\chi_{\text{sc}}^{\rho\rho}(\mathbf{k},\omega)[\Phi_{\text{pol}}(\mathbf{k},\omega)+\Phi_{\text{ext}}(\mathbf{k},\omega)]. \tag{5}$$

The density-density response function is defined as the strength of the system response to Φ_{ext} alone,

$$\langle\rho(\mathbf{k},\omega)\rangle=\chi(\mathbf{k},\omega)\Phi_{\text{ext}}(\mathbf{k},\omega), \tag{6}$$

and from Eqs. (4)–(6) it follows that

$$\chi(\mathbf{k},\omega)=\frac{\chi_{\text{sc}}^{\rho\rho}(\mathbf{k},\omega)}{1-f_k^s\chi_{\text{sc}}^{\rho\rho}(\mathbf{k},\omega)}. \tag{7}$$

In a system without backflow and without contributions from the multiphonon excitations, $\chi_{\text{sc}}^{\rho\rho}$ contains pairs of free particles excited from the condensate,

$$\chi_{\text{sc}}^{\rho\rho}(\mathbf{k},\omega)=\frac{\rho\hbar^2\mathbf{k}^2/m}{\hbar^2\omega^2-\hbar^4\mathbf{k}^4/4m^2}, \tag{8}$$

where ρ is the density. The density-fluctuation spectrum is found in the poles of χ and is given as

$$\hbar\omega=\left[\frac{\hbar^4\mathbf{k}^4}{4m^2}+\rho\frac{\hbar^2\mathbf{k}^2f_k^s}{m}\right]^{1/2}. \tag{9}$$

This is none other than the Bogoliubov spectrum with f_k^s replacing $V(k)$ in Eq. (3). f_k^s is interpreted as the effective interaction between atoms in the liquid and it is assumed that short-range correlations renormalize the hard core in the interaction to a soft core. This is equivalent to the extended Bogoliubov approximation used by Sobnack *et al.*[20]

Aldrich and Pines[27] introduced a mean field backflow effect into their theory by assuming that the density fluctuations are also affected by an additional vector polarization potential $\mathbf{A}_{\text{pol}}$, which couples to the current fluctuations $\mathbf{j}$ in the liquid,

$$\mathbf{A}_{\text{pol}}(\mathbf{k},\omega)=f_k^v\langle\mathbf{j}(\mathbf{k},\omega)\rangle. \tag{10}$$

The net response is then given by Eq. (5) with an additional term $\chi_{\text{sc}}^{\rho j}(\mathbf{k},\omega)A_{\text{pol}}(\mathbf{k},\omega)$ on the right-hand side. The continuity equation and the relationships between the correlation functions[33] give the density-density response function [Eq. (6)] as

$$\chi(\mathbf{k},\omega)=\frac{\chi_{\text{sc}}^{\rho\rho}(\mathbf{k},\omega)}{1-(f_k^s+\omega^2f_k^v/\mathbf{k}^2)\chi_{\text{sc}}^{\rho\rho}(\mathbf{k},\omega)}, \tag{11}$$

where the free-particle response function $\chi_{\text{sc}}^{\rho\rho}$ now has poles associated with pairs of free particles with a k-dependent effective mass m^*. Using the high-frequency limit of this density-density response function,[34] the vector polarization parameter f_v^k can be expressed in terms of the ''free''-particle effective mass m^*,

$$\rho f_k^v=m_k^*-m=\Delta m. \tag{12}$$

The strength of the backflow potential is thus proportional to the extra mass from the interaction, which is responsible for the backflow. The poles of the density response function χ then give the density fluctuation spectrum in the new approximation containing the backflow effect,

$$\hbar\omega=\left[\frac{\hbar^4\mathbf{k}^4}{4mm_k^*}+\rho\frac{\hbar^2\mathbf{k}^2f_k^s}{m}\right]^{1/2}. \tag{13}$$

C. Beliaev theory including the backflow effect

In the absence of backflow and multiphonon contributions, the PP theory reduces to the extended Bogoliubov approximation in the sense that the interaction term includes the short-range renormalized core, i.e., the interaction terms f_k^s and $V(k)$ are equivalent. When backflow is included in the PP theory, the single particle aquires an additional mass proportional to the strength of the coupling to the current fluctuations.

It is reasonable to expect[35] that one can derive a field theory incorporating the backflow based upon ''free'' particles, which have an effective mass m^* and define a new free-particle propagator G_0 accordingly,

$$G_0(\mathbf{k},\omega)=\left[\hbar\omega-\left(\frac{\hbar^2\mathbf{k}^2}{2m_k^*}-\mu\right)+i\delta\right]^{-1}. \tag{14}$$

This Green's function however is not a ''true'' free-particle Green's function in the sense that its poles are no longer the bare free particles. That is, we are using a ''backflow'' quasiparticle as the basis of our field theory. A truly microscopic theory would require a derivation of the effective mass parameter from first principles and the true G_0 would contain poles that were free particles. Equation (12), however, ensures that the pole will be a single bare atom when the density ρ is zero. The theory, therefore, has the correct end points in density.

The second effect of the introduction of backflow in the PP theory is to replace[35] the interaction f_k^s with

$$f_k^s+\frac{\omega^2}{\mathbf{k}^2}f_k^v.$$

One then finds that with the approximations

$$\Sigma_{11}=\rho\left(V(\mathbf{k})+\frac{\omega^2}{\mathbf{k}^2}f_k^v\right)+\rho\left(V(0)+\lim_{\omega,\mathbf{k}\to0}\frac{\omega^2}{\mathbf{k}^2}f_k^v\right),$$
$$\Sigma_{20}=\Sigma_{02}=\rho\left(V(\mathbf{k})+\frac{\omega^2}{\mathbf{k}^2}f_k^v\right), \tag{15}$$

for the self-energies, along with Eq. (14), the poles of F and G will then be equivalent to Eq. (13). These approximations, together with Eq. (15), are, therefore, equivalent to those of Aldrich and Pines including backflow and neglecting multiphonon contributions, due to the fact that the poles of F, G, and χ coincide—all correlation functions have coincidental poles within an equivalent order of approximation in Bose systems.[36] The quasiparticles of the system are now noninteracting quasiparticles that contain the backflow contribution.

The main effect of the m^* term in the excitation spectrum [Eq. (13)], is to lower the roton minimum in energy, leaving the maxon energy largely unaffected. In the original PP theory, a good fit to the experimental spectrum is found by including multiphonon contributions. Our objective here is to examine solely the effect of backflow and we deliberately neglect this contribution. We find that Eq. (13), with the potential[32] $V_0k^{-1}\sin(a_0k)$, with $V_0=15.2$ K Å^{-1} and $a_0=2.1$ Å, for f_k^s and $m_k^*=1.4m$, gives a very good fit to the experimental spectrum.[29] For simplicity, we take m^* to be k independent.

With the inclusion of the backflow potential $\hbar^2\omega^2W(\mathbf{k})$, where $W(\mathbf{k})=\Delta m/\hbar^2\mathbf{k}^2$, the two Beliaev ''coupled diagrams'' for the two propagators $G(\mathbf{k},\omega)$ and $F(\mathbf{k},\omega)$ of the superfluid ^{4}He system give, in real space, the equations of motion

$$\left[\hbar\omega-\mu(\mathbf{r})+\frac{\hbar^2}{2m^*}\nabla^2\right]\phi(\mathbf{r})-\int_{-\infty}^{+\infty}[\sqrt{\rho(\mathbf{r})}V(\mathbf{r}-\mathbf{r}')\sqrt{\rho(\mathbf{r}')}+\hbar^2\omega^2W(\mathbf{r}-\mathbf{r}')][\phi(\mathbf{r}')+\psi(\mathbf{r}')]d^3\mathbf{r}'=0,$$
$$\left[-\hbar\omega+\mu(\mathbf{r})+\frac{\hbar^2}{2m^*}\nabla^2\right]\psi(\mathbf{r})-\int_{-\infty}^{+\infty}[\sqrt{\rho(\mathbf{r})}V(\mathbf{r}-\mathbf{r}')\sqrt{\rho(\mathbf{r}')}+\hbar^2\omega^2W(\mathbf{r}-\mathbf{r}')]\times[\phi(\mathbf{r}')+\psi(\mathbf{r}')]d^3\mathbf{r}'=0 \tag{16}$$

for the ''particle-hole'' wave function $\phi(\mathbf{r})$ (associated with G) and the ''hole-particle'' wave function $\psi(\mathbf{r})$ (associated with F) valid in bulk, through the surface and in the vacuum.

As before,[20,22] the function $\mu(\mathbf{r})$ describes the variation of the binding energy. It changes from 0 (in bulk) to $|\mu_0|$ (in the vacuum) across the surface. $\mu_0=-7.16$ K is the condensate chemical potential. In deriving the above equations, we have allowed the condensate density $\rho(\mathbf{r})$ to vary with position so that the equations may be used to tackle the general inhomogeneous problem such as the free surface. Deep in the bulk, the density has the value of bulk superfluid condensate, i.e., $\rho=\rho_0$ (constant), and high above the surface it has the vacuum value $\rho=0$. We take $m^*=m+\Delta m\rho(\mathbf{r})/\rho_0$. The equations then are the Schrödinger equations for the quasiparticles (of energy $\hbar\omega$) in bulk, and in the vacuum the Schrödinger equations for the free atom (of energy $\hbar\omega-|\mu_0|$).

III. SOLUTION OF THE EQUATIONS AND RESULTS

Because the surface scattering processes conserve momentum parallel to the surface, the density profile $\rho(\mathbf{r})$ depends only on z, the component of $\mathbf{r}=(\mathbf{R},z)$ normal to the interface, i.e., $\rho=\rho(z)$. We give the quasiparticles a momentum $\hbar\mathbf{Q}$ parallel to the surface and look for solutions of the form

$$\phi(\mathbf{r})=e^{i\mathbf{Q}\cdot\mathbf{R}}\phi(z) \quad \text{and} \quad \psi(\mathbf{r})=e^{i\mathbf{Q}\cdot\mathbf{R}}\psi(z),$$

where $\mathbf{R}=(x,y)$. This reduces Eqs. (16) to the one-dimensional equations

$$\left[\hbar\omega-\mu(z)-\alpha\mathbf{Q}^2+\alpha\frac{d^2}{dz^2}\right]\phi(z)$$
$$-\int\left[\sqrt{\rho(z)}V(\mathbf{Q},z-z')\sqrt{\rho(z')}+\hbar^2\omega^2W(\mathbf{Q},z-z')\right]$$
$$\times[\phi(z')+\psi(z')]dz'=0, \quad (17)$$

$$\left[-\hbar\omega+\mu(z)-\alpha\mathbf{Q}^2+\alpha\frac{d^2}{dz^2}\right]\psi(z)$$
$$-\int\left[\sqrt{\rho(z)}V(\mathbf{Q},z-z')\sqrt{\rho(z')}+\hbar^2\omega^2W(\mathbf{Q},z-z')\right]$$
$$\times[\phi(z')+\psi(z')]dz'=0,$$

where $\alpha=\hbar^2/2m^*$. V has the same functional form as in Ref. 20, but now $V_0=15.2$ K Å^{-1} and $a_0=2.1$ Å. The backflow potential $\hbar^2\omega^2W$ takes the form

$$W(\mathbf{Q},z-z')=\frac{\Delta m}{\hbar^2}\frac{\exp-Q|z-z'|}{2Q},$$

where $Q=|\mathbf{Q}|$.

$\mu(z)=|\mu_0|f(z)$ gives the variation in the binding energy as discussed in Ref. 20. As before, we solve the equations of motion for $\phi(z)$ and $\psi(z)$ numerically in a box of size $2L$ $(-L+s\leqslant z\leqslant L+s$, with the surface centered at $z=0$ and bulk helium in $z<0)$ for a given energy $\hbar\omega$ and either for fixed parallel momentum $\hbar\mathbf{Q}$ or for fixed angle of incidence $\theta_{\rm in}$ using a fermi function for the surface profile $\rho(z)$ and taking the surface to have a 90%–10% width of 6.5 Å.[37]

A numerical procedure is used to extract the (real) amplitudes ϕ_i and ψ_i $[i=p$ (phonons), $-$ $(R^-$ rotons), $+$ $(R^+$ rotons), a (atoms)] of the wave functions of the various quasiparticles i and these are used to calculate the current $\mathbf{j}_i$ associated with each quasiparticle/atom from

$$\mathbf{j}_i=\frac{1}{2}\mathbf{v}_i(\phi_i^2-\psi_i^2), \quad (18)$$

where, because of the energy-dependent backflow potential $\hbar^2\omega^2W$, $\mathbf{v}_i$ has the definition

$$\mathbf{v}_i=\frac{m}{m^*}\nabla_{\mathbf{k}}\omega(\mathbf{k}) \quad (19)$$

instead of the usual group velocity $\mathbf{v}_i^g=\nabla_{\mathbf{k}}\omega(\mathbf{k})$ for the total quasiparticle current $\Sigma_i\mathbf{j}_i(i=p,-,+)$ to be conserved (see the Appendix). For the free atoms $(m=m^*)$, $\mathbf{v}_a=\hbar\mathbf{k}_a/m$. The currents are then used to calculate the probabilities of the various one-to-one surface scattering processes (see, for example, Ref. 17).

We have calculated the scattering rates P_{ij} (probability of state i scattering into state j) as a function of energy for various fixed parallel wave vectors and angles of incidence. We present some of our results below.

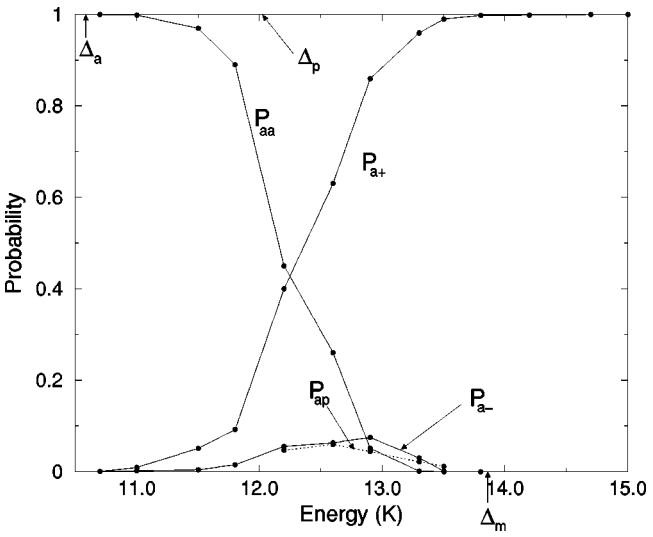

FIG. 1. The probabilities P_{aj} as a function of bulk energy for an atom incident on the free surface with a parallel wave vector $|\mathbf{Q}|=0.75$ Å^{-1}. Δ_a, Δ_p, and Δ_m are, respectively, the atom threshold, the phonon threshold, and the maxon energy.

A. Fixed parallel momenta

Figures 1–3 show the calculated probabilities P_{ij} as a function of energy (relative to the zero in bulk) of the different transitions available to atoms, R^- rotons, and R^+ rotons incident on the free surface with a fixed parallel wave vector $|\mathbf{Q}|=0.75$ Å. Conservation of energy and parallel momentum exclude phonons from the scattering processes for all energies less than the phonon threshold $\Delta_p=12.1$ K. Similarly there is a cutoff for atom states at $\Delta_a=10.6$ K (relative to bulk). These figures are the same as in Refs. 28–30 but are included here for completeness. We only summarize the main results here. The corresponding results without backflow are given in Figs. 8, 9 and 10 of Ref. 20. Figure 4 compares the probabilities P_{aj} $(j=a,-,+)$ presented in this study with those obtained without backflow (Ref. 20).

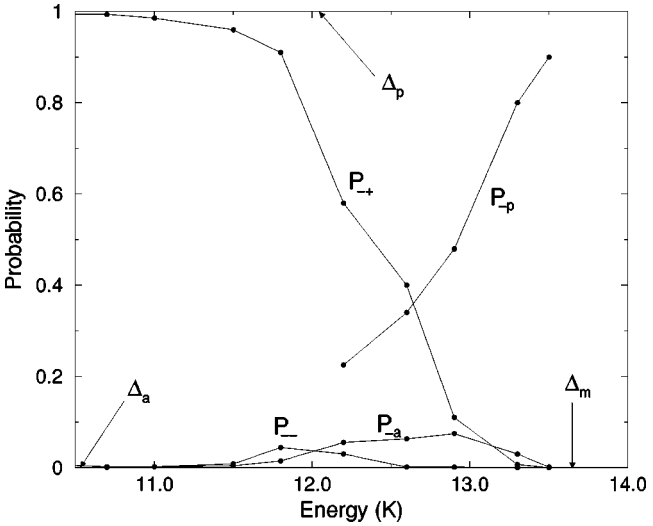

FIG. 2. The probabilities P_{-j} as a function of energy for an incident R^- roton. $|\mathbf{Q}|=0.75$ Å^{-1}.

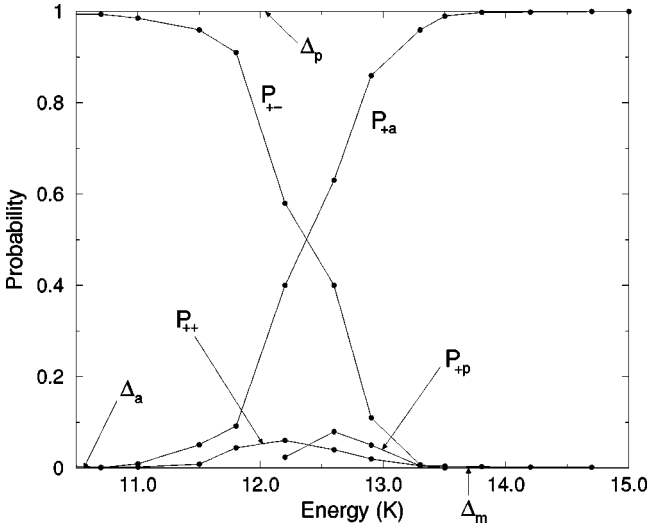

FIG. 3. The probabilities P_{+j} as a function of energy for an incident R^+ roton. $|\mathbf{Q}|=0.75$ Å^{-1}.

Backflow increases the probability P_{a+} of atoms condensing as R^+ rotons at all energies between the roton minimum Δ and the maxon Δ_m (Figs. 1 and 4); decreases the atomic reflectivity P_{aa} so that P_{aa} now decreases much faster as a function of energy (Figs. 1 and 4); decreases the specular reflectivity P_{--} of R^- rotons incident on the surface (Fig. 2); decreases the probability P_{-a} of R^- rotons evaporating atoms at all energies, but P_{-a} is finite (Fig. 2); considerably increases the probability P_{+a} $(=P_{+a})$ of R^+ rotons quantum evaporating (Figs. 3 and 4). The last two features suggest that with backflow included, the ratio P_{-a}/P_{+a} is considerably reduced, as indeed is clear from Fig. 4, more in line with the experimental estimates of Tucker and Wyatt.[38]

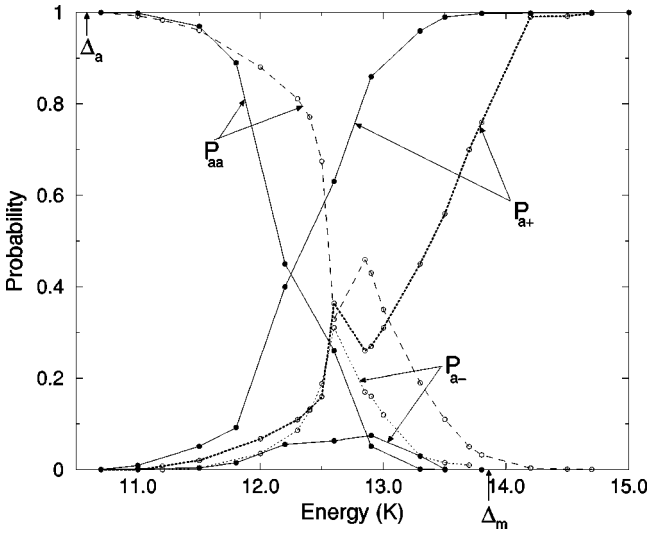

FIG. 4. The probabilities P_{aj} as a function of energy for an incident atom. $|\mathbf{Q}|=0.75$ Å^{-1}. Solid lines, with backflow included (as in Fig. 1); dashed lines, without backflow (Ref. 20)

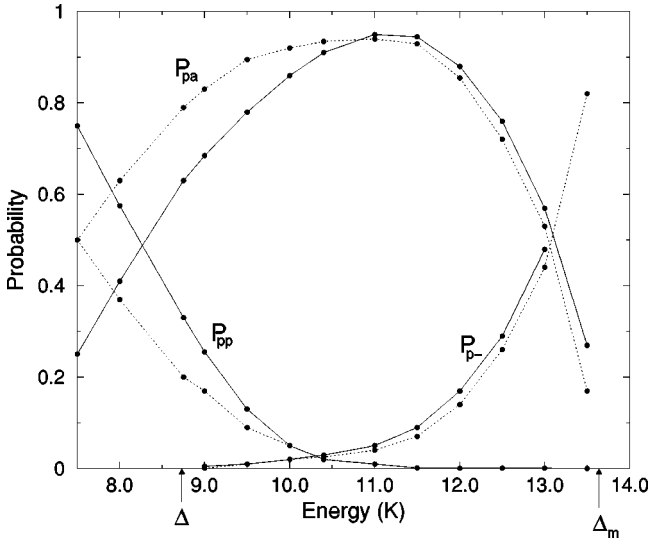

FIG. 5. The various scattering probabilities P_{pj} as a function of bulk energy for a phonon incident on the surface at $\theta_{\rm in}=14°$ (dotted lines) and $\theta_{\rm in}=25°$ (solid lines). Δ and Δ_m are the roton minimum energy and the maxon energy, respectively.

B. Fixed angles of incidence

To enable comparison with experiments on quantum evaporation we have calculated the scattering probabilities P_{ij} for fixed angles of incidence $\theta_{\rm in}$. In these experiments, the bolometer producing the quasiparticles is fixed at a given position in bulk helium and the beam of quasiparticles produced is collimated so that all the bulk excitations are incident on the surface at the same (fixed) angle. For a fixed angle of incidence $\theta_{\rm in}$, different excitations incident on the surface have different parallel momenta $\hbar\mathbf{Q}(\theta_{\rm in},\hbar\omega)$.

Figures 5, 6, and 7, respectively, give the calculated probabilities for phonons, R^- rotons, and R^+ rotons incident at $\theta_{\rm in}=14°$ (dotted lines) and $\theta_{\rm in}=25°$ (solid lines). $\Delta\sim 8.7$ K and $\Delta_m\sim 13.7$ K are the roton minimum and maxon energies. $\Delta_{-a}(25°)$ and $\Delta_{-p}(25°)$ are the atom and phonon thresholds for R^- coming in at 25°, and similarly, R^+ rotons incident at 25° cannot evaporate atoms at energies less than $\Delta_{+a}(25°)$ and cannot reflect as phonons for energies less than $\Delta_{+p}(25°)$.

As for the case when backflow is neglected, the results show that the calculated probabilities have a definite angular dependence, contrary to some of the other studies.[19] In particular, the probability P_{pp} of a phonon reflecting as a phonon or the probability P_{pa} of evaporating an atom depends quite strongly on the angle of incidence for energies up to about 11 K (Fig. 5). The mode change from reflection phonon to R^- roton, however, is independent of the angle of incidence—the change in (normal) momentum involved in this reflection does not depend very strongly on the angle of incidence.

For incident R^- rotons (Fig. 6), the probability of reflecting as a phonon is essentially independent of the angle of incidence. The probability of an R^- roton quantum evaporating depends strongly on the incident angle: at 12.0 K, for example, R^- rotons are about four times as likely to evapo-

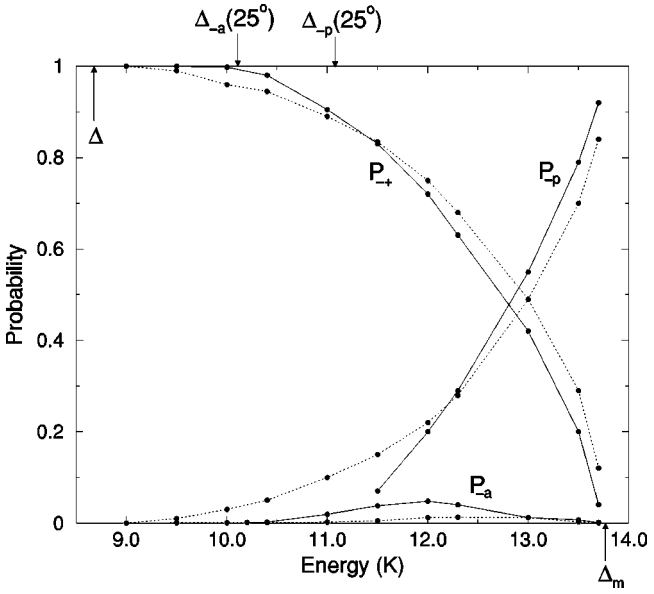

FIG. 6. The various scattering probabilities P_{-j} as a function of bulk energy for an R^- roton incident on the surface at $\theta_{\rm in}=14°$ (dotted lines) and $\theta_{\rm in}=25°$ (solid lines). $\Delta_{-a}(25°)$ and $\Delta_{-p}(25°)$ are, respectively, the atom and phonon threshold when R^- rotons are incident at 25°. Δ and Δ_m are the roton minimum energy and the maxon energy, respectively.

rate atoms at 25° than at 14°. Again, we find that, just as for fixed parallel momenta, the probability of evaporation by R^- rotons is smaller than when backflow is neglected (Fig. 13 of Ref. 20), but P_{-a} is still finite.

Direct comparison of Fig. 7 with Fig. 14 of Ref. 20 (as shown in Fig. 8, where we plot P_{+-} and P_{+a} for R^+ rotons

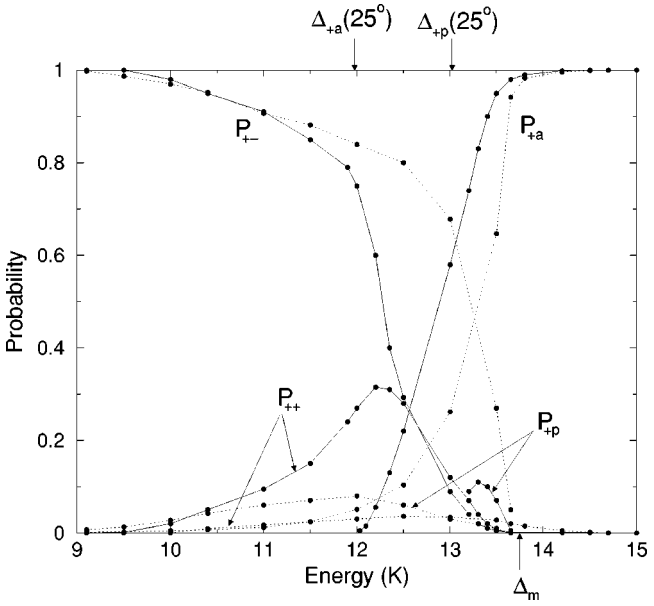

FIG. 7. The various scattering probabilities P_{+j} as a function of bulk energy for an R^+ roton incident on the surface at $\theta_{\rm in}=14°$ (dotted lines) and $\theta_{\rm in}=25°$ (solid lines). Δ_m is the maxon energy and $\Delta_{+a}(25°)$ and $\Delta_{+p}(25°)$ are, respectively, the atom and phonon threshold when R^+ rotons are incident at 25°.

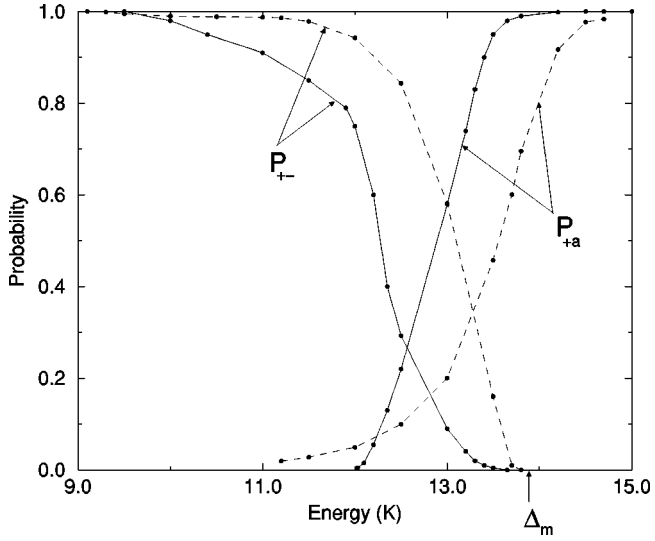

FIG. 8. The probabilities P_{+-} and P_{+a} for an R^+ roton incident on the surface at $\theta_{\rm in}=25°$. Solid lines, with backflow included (as in Fig. 1); dashed lines, without backflow (Ref. 20).

incident at $\theta_{\rm in}=25°$ calculated in this study with the corresponding probabilities calculated when backflow is neglected) shows that backflow has a large effect on the probabilities for incoming R^+ rotons: incident R^+ rotons are more efficient at quantum evaporating with backflow included, with, for example, at $\theta_{\rm in}=25°$, $P_{+a}\sim 0.6$ at $\hbar\omega=13.0$ K with backflow compared to $P_{+a}\sim 0.2$ without backflow. At all energies between $\Delta_{+a}(25°)$ and the maxon, backflow increases P_{+a} and the same result is true for R^+ rotons incident at 14° for all energies between the roton minimum and the maxon. Also, the mode change reflectivity P_{+-} decreases faster with energy with backflow included.

For incident R^+ rotons, the probabilities of all the possible transitions are strongly dependent on the angle of incidence. The probability P_{+-} of an R^+ roton reflecting as an R^- roton falls off more rapidly and the probability P_{+a} of quantum evaporation rises much faster with energy at 25° than at 14°. This is in sharp contrast with the scattering rates calculated when backflow is neglected. There the probability of quantum evaporation by R^+ rotons was independent of the angle of incidence.

Attempts to measure the absolute R^+ roton evaporation probabilities P_{+a} by indirect experiments[39–41] seem to suggest a value, typically ≈ 0.3, which increases with the wave vector. There have been no successful direct measurements because there is no independent method of determining the spectrum and flux of rotons generated by the pulsed thin-film heaters used in the experiments. However, the wave-vector (or energy) dependence of the evaporation probability predicted in this paper can be compared with the experiments of Brown and Wyatt[8] by using a detailed numerical simulation.[24,42] This assumes that the number density $n(q)$ of positive-group-velocity rotons generated with wave-vector magnitude q is

$$n_+(q)dq \propto \frac{q^\lambda dq}{\exp[\hbar\omega(q)/T_{\rm eff}-1]} \quad \text{with} \quad \lambda=2.$$

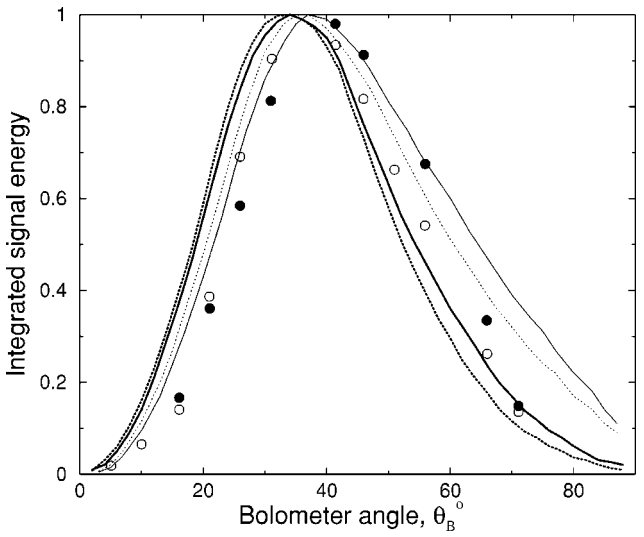

FIG. 9. The angular dependence of the $R^+ \rightarrow$atom signal energy, integrated up to 160 μs after the heater input pulse. The angle of incidence is $\theta_{in}=14°$. The experiments used two different heater powers, -24 dB (open circles) and -27 dB (full circles). The thin curves are simulations using $P_{+a}(q,\theta_{in})=$const. and the thick lines use the values reported in this work. The simulations use injected-roton spectra at two characteristic temperatures, $T_{eff}=1.0$ K (solid lines) and $T_{eff}=1.5$ K (dotted lines).

The shape of this distribution is dominated by the value of the parameter T_{eff} and is insensitive to the value of the density-of-states parameter for values $1 \leqslant \lambda \leqslant 3$. The value of the parameter T_{eff} is selected to fit the time-of-flight measurements—it increases with heater power and lies between 1.0 K and 1.5 K. It can be seen (see Fig. 9) that, for the present purposes, the simulation is not sensitive to the precise value of T_{eff}. The figure compares the measured angular distribution (circles) of atoms evaporated at $\theta_{in}=14°$ to the surface normal with R^+ roton evaporation measurements of Brown and co-workers,[8,42] with the simulations assuming a constant evaporation probability (thin lines) $P_{+a}(q,\theta_{in})=1$. The main features of Fig. 9 arise from the collimation geometry and the kinematics of quantum evaporation, but most significant for this paper is the fact that atoms detected at large values of the detector angle θ_B originate from R^+ rotons with relatively low energies. The measured values lie progressively below the simulation as θ_B increases above 40°, indicating that $P_{+a}(q,\theta_{in})$ increases with increasing q.

The thick lines in Fig. 9 are the results of using the probabilities P_{+a} for $\theta_{in}=14°$ calculated (shown in Fig. 7) using the theory described in this paper in the simulation. Comparison of this result with that presented in Fig. 14 of Ref. 20 shows that the agreement of the probabilities calculated in the present study with experiments is better as a result of including backflow. However, for evaporation angles less than 40°, there is a small, but obvious, discrepancy between simulation and experiment. This is because the theory cuts off the evaporation probability too sharply at low energies. This interpretation is confirmed by an analysis of the time-of-flight information, which will be presented elsewhere.[43]

IV. SUMMARY AND CONCLUDING REMARKS

It has long been recognized that roton backflow has to be included into any theory that deals with the dynamics of superfluid ^{4}He. In this paper, we have improved on the earlier theory of Sobnack and co-workers[20–22] by including backflow semiphenomenologically in the form of a backflow potential and calculated scattering rates for all the allowed one-to-one surface scattering processes as a function of energy, both for fixed parallel momenta and fixed angles of incidence.

The results show that backflow increases the evaporation efficiencies of R^+ rotons. In particular, at small roton energies, the efficiency of quantum evaporation by R^+ rotons is much larger with backflow included. The other salient effect of backflow is to decrease the probabilities P_{-a} of evaporation by R^- rotons, but P_{-a} is still nonzero at energies at which the conservation laws do not exclude phonons from the surface scattering processes, in agreement with experiments.[44] There are no measured probabilities with which to compare the efficiencies calculated in the present study. We have used the predicted $R^+ \rightarrow$atom evaporation probabilities P_{+a} in simulations of experiments, and a comparison of the calculated $R^+ \rightarrow$atom signal to the experimentally observed signal shows that including backflow improves the agreement of the scattering rates with experiments. However, the simulations also show that the theory still underestimates the efficiency of quantum evaporation by R^+ rotons at low roton wave vectors/energies.

There are limitations to the theory presented here, the main one being that it is not applicable at normal incidence. This is due to the fact that we have used a constant effective mass m^* [the backflow potential $\hbar^2\omega^2 W(\mathbf{Q},k)$ diverges in the limit $Q=|\mathbf{Q}|\rightarrow 0$], a restriction that needs to be removed by taking into account the k dependence of the vector polarization parameter f_v^k. Another limitation is that backflow in the sense of Aldrich and Pines, as we have used here, does not lead to phonon splitting and inelastic processes.

The work presented here is a study of one-to-one scattering processes. Liquid ^{4}He is a dynamic, many-body system and incoming particles may scatter into states other than the elastic channel. Recently, Campbell and co-workers[45] have studied the transmission of ^{4}He atoms through a helium slab and found that inelastic processes dominate the scattering—at around the roton minimum energy, the calculated signal has a sharp dip, showing that, at that energy, inelastic processes take up to about 90% of the energy of the incoming atoms.

Indeed, any realistic theory of the dynamics of quasiparticles in superfluid ^{4}He has to include a more rigorous inclusion of roton backflow and has to take into account inelastic processes (phonon decay processes, decay into the ripplon channels). Work along this direction is currently under way.

ACKNOWLEDGMENTS

M.B.S. would like to thank Professor F. V. Kusmartsev for useful discussions. M.B.S., J.R.M., and J.C.H.F. would like to acknowledge financial support from The Hong Kong Re-

search Grant Council, China (Project No. HKUST6080/98P), and J.R.M. and J.C.I. acknowledge financial support from the EPSRC. The authors would also like to thank Dr. M. Çakmak for help with the numerical work.

APPENDIX

In this appendix, we show that the current density is given by Eqs. (18) and (19). We follow Ref. 17. With the definition $\alpha=\hbar/2m^*$, Eqs. (16) takes the form

$$[\hbar\omega+\alpha\nabla^2]\phi(\mathbf{r})-\int_{-\infty}^{+\infty}[\rho V(\mathbf{r}-\mathbf{r}')+\hbar^2\omega^2 W(\mathbf{r}-\mathbf{r}')]\times[\phi(\mathbf{r}')+\psi(\mathbf{r}')]d^3\mathbf{r}'=0, \tag{A1}$$

$$[-\hbar\omega+\alpha\nabla^2]\psi(\mathbf{r})-\int_{-\infty}^{+\infty}[\rho V(\mathbf{r}-\mathbf{r}')+\hbar^2\omega^2 W(\mathbf{r}-\mathbf{r}')]\times[\phi(\mathbf{r}')+\psi(\mathbf{r}')]d^3\mathbf{r}'=0, \tag{A2}$$

well into the bulk, where the condensate density $\rho=$const and the function $\mu(\mathbf{r})=0$. Include a time dependence in the definitions of ϕ and ψ of the form

$$\phi(\mathbf{r},t)=\phi(\mathbf{r})e^{-i\omega t},\quad \psi(\mathbf{r},t)=\psi(\mathbf{r})e^{-i\omega t}. \tag{A3}$$

Then Eqs. (A1) and (A2) become, respectively,

$$-i\hbar\frac{\partial\phi}{\partial t}(\mathbf{r},t)=\alpha\nabla^2\phi(\mathbf{r})-\int_{-\infty}^{+\infty}[\rho V(\mathbf{r}-\mathbf{r}')+\hbar^2\omega^2 W(\mathbf{r}-\mathbf{r}')][\phi(\mathbf{r}',t)+\psi(\mathbf{r}')]d^3\mathbf{r}' \tag{A4}$$

and

$$i\hbar\frac{\partial\psi}{\partial t}(\mathbf{r},t)=\alpha\nabla^2\psi(\mathbf{r})-\int_{-\infty}^{+\infty}[\rho V(\mathbf{r}-\mathbf{r}')+\hbar^2\omega^2 W(\mathbf{r}-\mathbf{r}')]\times[\phi(\mathbf{r}')+\psi(\mathbf{r}')]d^3\mathbf{r}', \tag{A5}$$

where we have omitted the t dependence in the arguments of ϕ and ψ on the right-hand side. Next subtract $\phi^*(\mathbf{r},t)$ times Eq. (A4) from $\phi(\mathbf{r},t)$ times the complex conjugate of Eq. (A4), and similarly for Eq. (A5) and $\psi(\mathbf{r},t)$. Adding the resulting equations, one ends up with

$$\begin{aligned}i\hbar\frac{\partial}{\partial t}[|\phi(\mathbf{r},t)|^2-|\psi(\mathbf{r},t)|^2]&=\alpha\boldsymbol{\nabla}\cdot[\phi(\mathbf{r})\nabla\phi^*(\mathbf{r})-\phi^*(\mathbf{r})\nabla\phi(\mathbf{r})+\psi(\mathbf{r})\nabla\psi^*(\mathbf{r})\\&-\psi^*(\mathbf{r})\nabla\psi(\mathbf{r})]-\int_{-\infty}^{+\infty}[\rho V(\mathbf{r}-\mathbf{r}')+\hbar^2\omega^2 W(\mathbf{r}-\mathbf{r}')]\\&\times[\phi(\mathbf{r})\phi^*(\mathbf{r}')-\phi^*(\mathbf{r})\phi(\mathbf{r}')+\phi(\mathbf{r})\psi^*(\mathbf{r}')\\&-\phi^*(\mathbf{r})\psi(\mathbf{r}')+\psi(\mathbf{r})\phi^*(\mathbf{r}')-\psi^*(\mathbf{r})\phi(\mathbf{r}')\\&+\psi(\mathbf{r})\psi^*(\mathbf{r}')-\psi^*(\mathbf{r})\psi(\mathbf{r}')]d^3\mathbf{r}'.\end{aligned} \tag{A6}$$

$\phi(\mathbf{r},t)$ and $\phi(\mathbf{r},t)$ are plane waves, $\phi(\mathbf{r})=\phi e^{i\mathbf{k}\cdot\mathbf{r}}$ and $\psi(\mathbf{r})=\psi e^{i\mathbf{k}\cdot\mathbf{r}}$, so the kinetic term on the right-hand side of Eq. (A6) reduces to

$$-2i\alpha[|\phi|^2+|\psi|^2]\boldsymbol{\nabla}\cdot\mathbf{k}=-i\hbar\boldsymbol{\nabla}\cdot\mathbf{j}_{\rm kin}, \tag{A7}$$

where

$$\mathbf{j}_{\rm kin}=(|\phi|^2+|\psi|^2)\frac{\hbar}{m^*}\mathbf{k}. \tag{A8}$$

To deal with the terms involving the interactions, we use the Fourier decomposition

$$F(\mathbf{r})=\frac{1}{(2\pi)^3}\int F(\mathbf{k}')e^{i\mathbf{k}'\cdot\mathbf{r}}d^3\mathbf{k}' \tag{A9}$$

and take the limit $\phi(\mathbf{k}')=(2\pi)^3\phi\delta^{(3)}(\mathbf{k}'-\mathbf{k})$ at the end. We write the terms on the right-hand side of Eq. (A6) involving the interactions as

$$\begin{aligned}&\int_{-\infty}^{+\infty}[\rho V(\mathbf{r}-\mathbf{r}')+\hbar^2\omega^2 W(\mathbf{r}-\mathbf{r}')][\phi(\mathbf{r})\phi^*(\mathbf{r}')\\&-\phi^*(\mathbf{r})\phi(\mathbf{r}')+\phi(\mathbf{r})\psi^*(\mathbf{r}')-\phi^*(\mathbf{r})\psi(\mathbf{r}')\\&+\psi(\mathbf{r})\phi^*(\mathbf{r}')-\psi^*(\mathbf{r})\phi(\mathbf{r}')+\psi(\mathbf{r})\psi^*(\mathbf{r}')\\&-\psi^*(\mathbf{r})\psi(\mathbf{r}')]d^3\mathbf{r}'\\&=\frac{1}{(2\pi)^6}\int[\rho\{V(\mathbf{k}')-V(\mathbf{k}_1)\}\\&+\hbar^2\omega^2\{W(\mathbf{k}')-W(\mathbf{k}_1)\}]e^{i(\mathbf{k}_1-\mathbf{k}')\cdot\mathbf{r}}[\phi(\mathbf{k}_1)\phi^*(\mathbf{k}')\\&+\phi(\mathbf{k}_1)\psi^*(\mathbf{k}')+\psi(\mathbf{k}_1)\phi^*(\mathbf{k}')\\&+\psi(\mathbf{k}_1)\psi^*(\mathbf{k}')]d^3\mathbf{k}_1d^3\mathbf{k}'.\end{aligned} \tag{A10}$$

Now consider $\phi(\mathbf{k}_1)$ and $\psi(\mathbf{k}_1)$ as δ functions. Then the above reduces to

$$i\boldsymbol{\nabla}\cdot(\phi+\psi)(\phi^*+\psi^*)[\rho\nabla_{\mathbf{k}}V(\mathbf{k})+\hbar^2\omega^2\nabla_{\mathbf{k}}W(\mathbf{k})] \tag{A11}$$

and Eq. (A6) becomes

$$\begin{aligned}i\hbar\frac{\partial}{\partial t}[|\phi(\mathbf{r},t)|^2-|\psi(\mathbf{r},t)|^2]&=-i\hbar\boldsymbol{\nabla}\cdot\mathbf{j}_{\rm kin}-i\boldsymbol{\nabla}\cdot[(\phi+\psi)^2\{\rho\nabla_{\mathbf{k}}V(\mathbf{k})\\&+\hbar^2\omega^2\nabla_{\mathbf{k}}W(\mathbf{k})\}],\end{aligned} \tag{A12}$$

where we have assumed, without loss of generality, that ϕ and ψ are real. It is easily shown from Eqs. (A4) and (A5) that ϕ and ψ satisfy

$$\phi^2+\psi^2=\frac{m^*}{\hbar\omega\mathbf{k}^2}\left[\omega^2+\left(\frac{\hbar\mathbf{k}^2}{2m^*}\right)^2\right](\phi^2-\psi^2),$$

$$(\phi+\psi)^2=\frac{\hbar\mathbf{k}^2}{2m^*\omega}(\phi^2-\psi^2).$$

Using these together with the dispersion relation

$$\hbar^2\omega^2=\alpha^2\mathbf{k}^4+2\alpha\mathbf{k}^2[\rho V(\mathbf{k})+\hbar^2\omega^2 W(\mathbf{k})] \tag{A13}$$

gives, after some algebra,

$$i\hbar\frac{\partial}{\partial t}(\phi^2-\psi^2)=-i\hbar(\phi^2-\psi^2)\nabla\cdot\left[\left(1-\frac{\hbar^2\mathbf{k}^2}{m^*}W(\mathbf{k})\right)\nabla_{\mathbf{k}}\omega+\frac{1}{\mathbf{k}^2}\left(\omega-\frac{\hbar^2\mathbf{k}^4}{4m^{*2}\omega}-\frac{\mathbf{k}^2}{m^*\omega}[\rho V(\mathbf{k})+\hbar^2\omega^2W(\mathbf{k})]\right)\mathbf{k}\right]$$
$$=-i\hbar\nabla\cdot\left[1-\frac{\hbar^2\mathbf{k}^2}{m^*}W(\mathbf{k})\right](\phi^2-\psi^2)\nabla_{\mathbf{k}}\omega, \tag{A14}$$

where we have used the dispersion relation (A13). Hence, if we interpret

$$(\phi^2-\psi^2)=\varrho, \tag{A15}$$

as the density of elementary excitations, then ϱ satisfies the continuity equation

$$\frac{\partial}{\partial t}\varrho+\nabla\cdot\mathbf{j}^{\mathrm{ex}}=0, \tag{A16}$$

where the current density $\mathbf{j}^{\mathrm{ex}}$ is given by

$$\mathbf{j}^{\mathrm{ex}}=\mathbf{v}\varrho \tag{A17}$$

with

$$\mathbf{v}=\left[1-\frac{\hbar^2\mathbf{k}^2}{m^*}W(\mathbf{k})\right]\nabla_{\mathbf{k}}\omega=\frac{m}{m^*}\nabla_{\mathbf{k}}\omega, \tag{A18}$$

since $W(\mathbf{k})=(m^*-m)/\hbar^2\mathbf{k}^2$.

[1] P.L. Kapitza, Nature (London) **141**, 74 (1932).
[2] L.D. Landau, J. Phys. (Moscow) **5**, 71 (1941).
[3] H. Palevsky, K. Otnes, and K.E. Larsson, Phys. Rev. **112**, 11 (1958).
[4] W.D. Johnston, Jr. and J.C. King, Phys. Rev. Lett. **16**, 1191 (1966).
[5] S. Balibar, J. Buechner, B. Castaing, C. Laroche, and A. Libchaber, Phys. Rev. B **18**, 3096 (1977).
[6] M.J. Baird, F.R. Hope, and A.F.G. Wyatt, Nature (London) **304**, 325 (1983).
[7] A.F.G. Wyatt, Physica A **126B**, 392 (1984).
[8] M. Brown and A.F.G. Wyatt, J. Phys.: Condens. Matter **2**, 5025 (1990).
[9] G.M. Wyborn and A.F.G. Wyatt, Jpn. J. Appl. Phys., Suppl. **26-3**, 2095 (1987).
[10] A.F.G. Wyatt, in *Phonons '89*, edited by S. Hunklinger, W. Ludwig, and G. Weiss (World Scientific, Singapore, 1990), p. 1019.
[11] D.S. Hyman, M.O. Scully, and A. Widom, Phys. Rev. **186**, 231 (1969).
[12] A. Griffin, Phys. Lett. **31A**, 222 (1970).
[13] M.W. Cole, Phys. Rev. Lett. **28**, 1622 (1972).
[14] H.J. Maris, J. Low Temp. Phys. **87**, 773 (1992).
[15] P.A. Mulheran and J.C. Inkson, Phys. Rev. B **46**, 5454 (1992).
[16] F. Dalfovo, A. Fracchetti, A. Lastri, L. Pitaevskii, and S. Stringari, Phys. Rev. Lett. **75**, 2510 (1995).
[17] F. Dalfovo, A. Fracchetti, A. Lastri, L. Pitaevskii, and S. Stringari, J. Low Temp. Phys. **104**, 367 (1996).
[18] S. Stringari, F. Dalfovo, M. Guilleumas, A. Lastri, and L. Pitaevskii, Czech. J. Phys. **46-S6**, 2973 (1996).
[19] M. Guilleumas, F. Dalfovo, I. Oberosler, L. Pitaevskii, and S. Stringari, J. Low Temp. Phys. **110**, 449 (1998).
[20] M.B. Sobnack, J.C. Inkson, and J.C.H. Fung, Phys. Rev. B **60**, 3465 (1999).
[21] M.B. Sobnack and J.C. Inkson, Phys. Rev. B **56**, R14 271 (1997).
[22] M.B. Sobnack and J.C. Inkson, Phys. Rev. Lett. **82**, 3657 (1999).
[23] S.T. Beliaev, Sov. Phys. JETP **7**, 289 (1958).
[24] C.D.H. Williams, J. Low Temp. Phys. **113**, 627 (1998).
[25] R.P. Feynman and M. Cohen, Phys. Rev. **102**, 1189 (1956).
[26] R.P. Feynman, Phys. Rev. **94**, 262 (1954).
[27] C.H. Aldrich and D. Pines, J. Low Temp. Phys. **25**, 677 (1976).
[28] M.B. Sobnack, Phys. Rev. B **62**, 11 355 (2000).
[29] J.R. Matthias, M.B. Sobnack, J.C. Inkson, and J.C.H. Fung, J. Low Temp. Phys. **121**, 345 (2000).
[30] M.B. Sobnack, J.R. Matthias, and J.C.H. Fung, J. Low Temp. Phys. **121**, 339 (2000).
[31] N.N. Bogoliubov, J. Phys. (Moscow) **11**, 23 (1947).
[32] K.A. Brueckner and K. Sawada, Phys. Rev. **106**, 1117 (1957); **106**, 1128 (1957).
[33] A. Griffin, *Excitations in a Bose Condensed Liquid* (Cambridge University Press, Cambridge, England, 1994).
[34] D. Pines, in *Quantum Fluids* edited by D. Brewer (North-Holland, Amsterdam, 1966).
[35] J.R. Matthias, Ph.D. thesis, University of Exeter, 1998.
[36] P.C. Hohenberg and P.C. Martin, Phys. Rev. Lett. **12**, 69 (1964).
[37] D.V. Osborne, J. Phys.: Condens. Matter **1**, 289 (1989).
[38] M.A.H. Tucker and A.F.G. Wyatt, J. Low Temp. Phys. **113**, 615 (1998).
[39] P. Fozooni, D.S. Spencer, and M. Lea, Jpn. J. Appl. Phys., Part 1 **26**, 26 (1987).
[40] C. Enss, S.R. Bandler, R.E. Lanou, H.J. Maris, T. More, F.S. Porter, and G.M. Siedel, Physica B **194**, 515 (1994).
[41] A.C. Forbes and A.F.G. Wyatt, J. Low Temp. Phys. **101**, 537 (1995).
[42] C.D.H. Williams, J. Low Temp. Phys. **113**, 11 (1998).
[43] C.D.H. Williams and M.B. Sobnack, J. Low. Temp. Phys. **126**, 603 (2002).
[44] M.A.H. Tucker and A.F.G. Wyatt, J. Low Temp. Phys. **121**, 333 (2000).
[45] C.E. Campbell, E. Krotscheck, and M. Saarela, Phys. Rev. Lett. **80**, 2169 (1998).